Tuijin Jishu/Journal of Propulsion Technology
ISSN: 1001-4055
Vol. 44 No. 3 (2023)

Real Time Voltage Stability Estimation under Contingencies by Generalized Curve Fit Method using PMU

[1]Padmesh Singh, [2]Awadhesh Kumar, [3]Surya Bhushan Dubey, [4]Pankaj Sahu
[1]Madan Mohan Malaviya University of Technology, Gorakhpur, India
[2]Madan Mohan Malaviya University of Technology, Gorakhpur, India
[3]SR Group of Institution Lucknow, India
[4]SR Group of Institution Lucknow, India

***Abstract*—**An accurate voltage stability monitoring scheme is necessary to take possible remedial action. Recent developments in Phasor Measurement Units (PMUs) technology provide the foundation for online voltage stability monitoring of a power system network. In this paper, the generalized curve fit method using PMUs in the system has been used to access voltage stability of the system and a sensitivity based approach has been used to identify critical buses of the system. Voltage stability margin has been obtained and compared using generalized curve fit method and continuation power flow method using PMUs in the system. Variations in voltage stability margin caused by changing load patterns have also been considered while estimating voltage stability under contingencies. Nose curves obtained using generalized curve fit and continuation power flow methods are also compared. Case studies have been performed on a standard IEEE 14-bus system and practical 246-bus Northern Regional Power Grid (NRPG) system representing power network of nine states of India, with the help of Real Time Digital Simulation (RTDS) and Power System Analysis Toolbox (PSAT) software.

***Keywords*—** *Voltage stability, contingencies, generalized curve fit method, nose curves, optimal PMUs placement, observability.*

Introduction

PMUs have become an advanced technology through many advances around the world. Major blackouts in the world including North Belgium 1982, New York 1970, Tokyo 1987 and 2003 major blackouts in North America and Europe were caused by voltage instability and voltage collapse and intend us to use data obtained from PMUs. Because of severity and frequency of occurrence of these blackouts researchers have paid significant attention on the area of voltage instability. PMUs provide data at high sampling rate and alloys efficient monitoring of system voltages. Data provided by PMUs are accurate and enables system operators to find the correct sequence of events which leads to blackout. The use of PMU technology in improving monitoring, control and protection of power systems is well documented [1]. The continual growth in power demands has forced our interconnected grid system to operate closer to its limits. Nowadays supervisory control and data acquisition (SCADA) and energy management system (EMS) controls are conventional methods for voltage stability monitoring and control utilizing *P-V* and *Q-V* curves [2]. The development and applications of PMU technology has provides a base for online voltage stability monitoring and control. With the deployment and installation of PMUs in the power system network, there is an opportunity to explore new methods for voltage stability monitoring. A voltage stability index utilizing data obtained from phasor measurements is used to find critical buses and a new parallel optimization method has been used to increase voltage stability margin of the system [3]. However, in this paper locations of PMUs in the system have not been shown.

Voltage stability monitoring methods using PMU measurements are mainly classified as the methods based upon Thevenin equivalent (TE) [4] or its derivations [5] the power network and sensitivity based methods [6-7]. The determination of TE parameters of an interconnected power system network are essential for the methods based upon TE and a core algorithm is used to determine voltage stability margin of the system. Several methods [8, 9] have been reported for online estimation of TE parameters of the power system network using PMU measurements. Fengkai Hu et al in [10] proposed a measurement based voltage stability monitoring method for a load area fed by N tie lines. As compared to conventional TE methods this method creates N+1 buses equivalent system to monitor and model each tie line. Therefore, using this methodology real power transfer limit of each tie line can be calculated using PMU data. However, TE based methods are valid for linear approximation of power system networks. In [11], Q-V sensitivity based approaches have been proposed using PMU data.

The continuation power flow method is used to find V-λ curve and critical point (voltage collapse point) is found using predictor and corrector step [12, 13]. The modal based method has been used to find the point of collapse using Jacobian matrix [14]. This Jacobian matrix becomes singular at the point of collapse. The centralized voltage stability methods proposed in [7, 15-16] may not work well in time when associated with large number of variables and in case of limit-induced bifurcations.

The voltage instability monitoring and protection method using local identification of global voltage instability (LIVES) has been applied to several IEEE test systems for voltage stability assessment [17]. It provides a LIVES alarms in case of voltage being unstable. Yiwei Qiu et al in [18] proposed a method for globally approximating static voltage stability region boundaries of power systems. They applied parametric polynomial approximation to the criterion equation which defines the static voltage stability region boundaries. Techniques in [17, 18] do not require system observability through PMU measurements as PMU technology is ambitious and definitely requires advanced infrastructure which is yet not available in practice. G.C. Ejebe et al in [19] proposed various methods including generalized curve fit method for voltage stability analysis of power systems without using PMUs in the system.

In this paper, generalized curve fit method utilizing the data obtained from PMUs is used to access voltage stability of the system. It is seen that generalized curve fit method has better performance in terms of voltage stability margin as compared to conventional continuation power flow based approach. Case studies have been carried out on a standard IEEE 14-bus system and a practical 246-bus North Region Power Grid (NRPG) system of India [20].

The paper has been structured as follows: Section II presents proposed generalized curve fit approach for determination of voltage stability margin under different operating scenarios using measurements obtained from PMUs section III proposes and validates effectiveness of generalized curve fit approach using PMUs in the system in estimation of voltage stability margin under different operating conditions, through case studies performed on two test systems considered.

Proposed Generalized Curve Fit Method For Voltage Stability Assessment Using PMU In The System

In this method an approximation of the nose curve is determined to find the voltage stability margin of the system. In this method stable branch of nose curve is computed and an approximation of the critical point is obtained using a curve fitting technique. Figure 1 shows that the stable branch of nose curves (i.e. V-λ curve: considered in this work) obtained using continuation power flow method can be approximated by a second order polynomial.

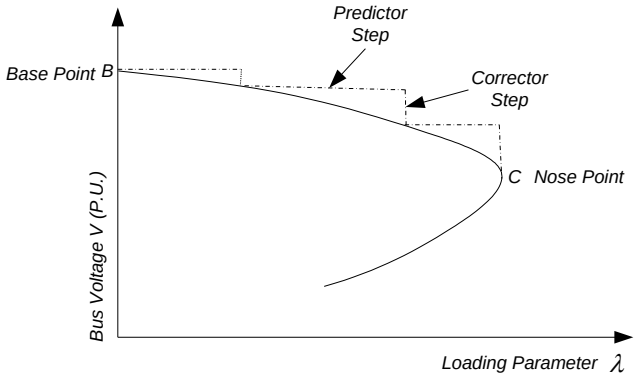

Figure 1: Nose curve (*V*-*λ* curve) obtained using continuation power flow method

To fit a desired second order polynomial it is sufficient to determine three stable equilibrium points on the curve. One of these points corresponds to the base case loading λ equal to zero ($\lambda = 0$) and is denoted by $(V^{(1)}, \lambda^{(1)})$. The other two points can be computed by increasing the loading parameter λ such that $\lambda^{(3)} > \lambda^{(2)} > \lambda^{(1)}$. The points corresponding to $(V^{(2)}, \lambda^{(2)})$ and $(V^{(3)}, \lambda^{(3)})$ can be obtained using two steps of continuation power flow method as shown in Figure 1.

The three points $(V^{(1)}, \lambda^{(1)})$, $(V^{(2)}, \lambda^{(2)})$ and $(V^{(3)}, \lambda^{(3)})$ are then used to fit the approximate stable branch:

$$\lambda_k = a_{1k}(V_k)^2 + a_{2k}V_k + a_{3k} \tag{7}$$

The constants a_1, a_2 and a_3 are then computed by solving the set of following linear equations:

$$\lambda_k^{(1)} = a_{1k}(V_k^{(1)})^2 + a_{2k}V_k^{(1)} + a_{3k} \tag{8}$$

$$\lambda_k^{(2)} = a_{1k}(V_k^{(2)})^2 + a_{2k}V_k^{(2)} + a_{3k} \tag{9}$$

$$\lambda_k^{(3)} = a_{1k}(V_k^{(3)})^2 + a_{2k}V_k^{(3)} + a_{3k} \tag{10}$$

After the evaluation of approximate stable branch, the voltage collapse point is given by:

$$\frac{dV_k}{d\lambda_k} = -\frac{a_{2k}}{2a_{1k}},\ k = 1, 2, ..., n_c \tag{11}$$

Maximum loadability limit $\lambda_{\max}$ (defined as voltage stability margin in this work), is given by:

$$\lambda_{\max_k} = -\frac{(a_{2k})^2}{4a_{1k}} + a_{3k} \tag{12}$$

where, *k* stands for a load bus of the power system network

In this work, nose curves (V-λ) of critical buses is obtained using the continuation power flow method in Power System Analysis Toolbox (PSAT) with PMUs optimally placed in the system. Then three points on this curve are used to fit a second order polynomial for voltage stability estimation. The first point of this curve corresponds to the base case loading λ equal to zero ($\lambda = 0$) while the other two points are obtained using two steps of continuation power flow method near but before critical point. The proposed generalized curve fit method utilizes these three points to obtain voltage stability margin of the system. The results have been verified on a standard IEEE 14-bus system and North Region Power Grid (NRPG) 246-bus system which are presented as shown below:

Case Studies

A. IEEE 14-Bus System [22]

IEEE 14-Bus System shown in Figure 2 has zero injection bus at bus number 7, generators at buses 1 and 2 and synchronous condensers at buses 3, 6 and 8. This system has 20 transmission lines including 3 transformers. Top three critical contingencies for IEEE 14-Bus System are 1-2, 2-3, 5-6 and critical buses of the system are 4, 5, 9, 10, 13 and 14. In Power System Analysis Toolbox (PSAT) and Real Time Digital Simulation (RTDS) five PMUs at buses 2, 4, 5, 6 and 9 were optimally placed in the system using binary integer linear programming considering wide pattern of load variations (viz. k=0.2, 0.5, 1.0, and 1.2) [21].

Tables I, II, III and IV show the results of voltage stability margin of the system obtained under different patterns of load variations (viz. k=0.2, 0.5, 1.0, and 1.2) for different critical buses of the system in a comparative manner using Power System Analysis Toolbox (PSAT) and Real Time Digital Simulation (RTDS). X_1, X_2, X_3 and X_4 are as defined in appendix B. An observation of Tables I, II, III and IV show that Voltage Stability Margins X_1 and X_2 obtained in Power System Analysis Toolbox (PSAT) match with each other for the critical buses 4, 5 and 9 in most of the cases. While these values differ marginally for critical buses 10, 13 and 14 considering wide pattern of load increase. Voltage Stability Margins X_3 and X_4 obtained in Real Time Digital Simulation (RTDS) are different. In generalized curve fit method the first point corresponds to base case point (λ=0) while the other two points are found using two steps of continuation power flow method near but before critical point. These three points for use in generalized curve fit method were obtained from nose curve (V-λ curve) by utilizing data obtained from pseudo-measurements and PMUs measurements by continuation power flow method using Power System Analysis Toolbox (PSAT).

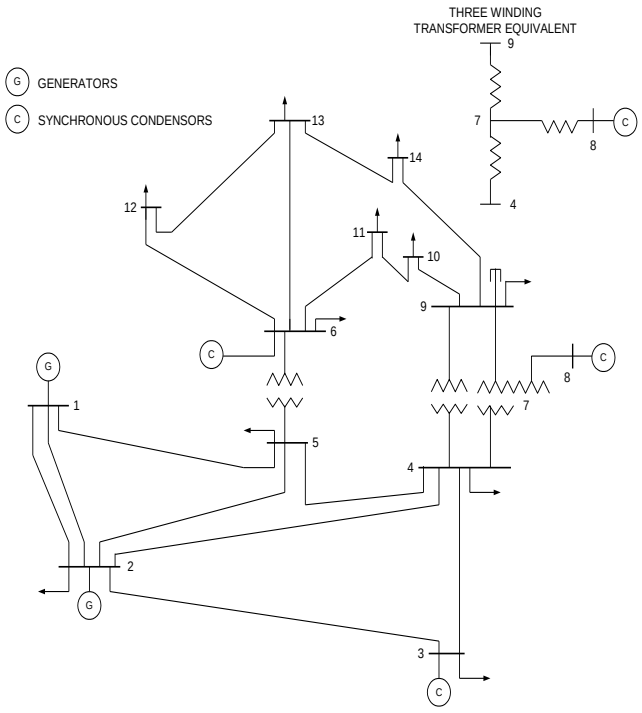

Figure 2: IEEE 14-Bus System

TABLE I
VOLTAGE STABILITY MARGINS COMPARISION FOR *k* = 0.2 IN IEEE 14-BUS SYSTEM

Critical Contingency	Critical Bus	X_1	X_2	X_3	X_4
Intact	4	5.26	5.37	17.27	10.02
	5	4.93	4.94	5.63	9.99
	9	5.31	5.32	9.95	7.89
	10	5.31	-	14.49	12.52
	13	5.31	11.51	18.54	11.19
	14	5.31	10.71	9.20	8.20
1-2	4	1.48	2.01	2.73	8.06
	5	1.33	1.31	1.88	1.39
	9	1.48	-	8.20	5.41
	10	1.48	17.62	8.78	21.60
	13	1.48	5.69	9.36	17.52
	14	1.48	8.72	3.94	6.53
2-3	4	2.99	2.92	2.62	3.33
	5	3.34	3.34	4.31	5.85
	9	3.66	3.70	4.32	6.57
	10	3.66	14.71	15.92	19.16
	13	3.66	6.93	26.59	19.80
	14	3.66	-	7.39	8.04
5-6	4	4.46	4.35	9.47	11.56
	5	4.61	4.47	10.73	7.14
	9	4.93	4.67	4.20	4.20
	10	4.94	5.25	11.84	11.84
	13	4.95	8.69	8.29	8.29
	14	4.91	5.20	4.51	6.90

TABLE II
VOLTAGE STABILITY MARGINS COMPARISION FOR *k* =0.5 IN IEEE 14-BUS SYSTEM

Critical Contingency	Critical Bus	X_1	X_2	X_3	X_4
Intact	4	5.26	5.38	10.82	9.51
	5	4.93	4.95	5.70	10.98
	9	5.31	5.63	8.97	5.61

	10	5.31	-	7.08	21.27
	13	5.31	12.68	8.21	24.35
	14	5.31	10.85	8.34	9.05
1-2	4	1.48	1.96	1.99	22.19
	5	1.34	1.34	1.71	2.69
	9	1.48	1.99	4.18	5.36
	10	1.48	-	5.33	19.86
	13	1.48	6.28	2.50	30.35
	14	1.48	9.15	2.06	5.99
2-3	4	2.99	2.97	4.12	10.60
	5	3.34	3.36	3.38	5.71
	9	3.66	4.14	8.39	5.22
	10	3.66	-	7.53	12.82
	13	3.66	7.41	4.72	20.07
	14	3.66	-	7.35	8.30
5-6	4	4.47	4.44	10.76	9.50
	5	4.61	4.58	14.46	6.55
	9	4.40	4.48	5.32	20.25
	10	4.94	5.29	12.97	14.90
	13	4.94	9.33	6.58	8.84
	14	4.90	5.19	6.71	6.55

TABLE III
VOLTAGE STABILITY MARGINS COMPARISION FOR *k* =1.0 IN IEEE 14-BUS SYSTEM

Critical Contingency	Critical Bus	X_1	X_2	X_3	X_4
Intact	4	4.64	4.71	8.63	7.08
	5	4.29	4.33	6.59	5.88
	9	4.67	5.43	4.80	9.22
	10	4.67	-	4.84	16.99
	13	4.67	12.93	13.05	18.98
	14	4.67	10.40	7.94	8.06
1-2	4	1.42	1.73	1.52	4.71
	5	1.33	1.15	1.50	1.94
	9	1.43	3.20	1.78	1.95
	10	1.43	-	3.41	12.8

					6
	13	1.43	6.78	4.29	25.69
	14	1.43	-	6.19	6.68
2-3	4	2.94	2.80	3.71	4.04
	5	3.34	2.97	3.78	9.19
	9	3.65	4.69	4.97	6.18
	10	3.65	-	9.10	16.05
	13	3.65	9.04	3.96	18.58
	14	3.65	-	7.36	7.70
5-6	4	4.48	4.27	5.37	9.70
	5	4.61	4.06	5.51	10.01
	9	4.27	4.27	7.70	4.84
	10	4.93	5.05	5.35	6.26
	13	4.94	9.84	8.94	9.48
	14	4.88	4.86	6.25	6.35

TABLE IV
VOLTAGE STABILITY MARGINS COMPARISION FOR *k* =1.2 IN IEEE 14-BUS SYSTEM

Critical Contingency	Critical Bus	X_1	X_2	X_3	X_4
Intact	4	5.26	5.37	9.53	7.99
	5	4.92	4.91	5.94	9.86
	9	5.30	6.28	5.74	36.72
	10	5.31	-	11.28	16.86
	13	5.31	13.20	6.00	16.78
	14	5.31	10.47	7.59	7.90
1-2	4	1.48	1.92	1.43	2.11
	5	1.33	1.31	1.30	1.69
	9	1.48	3.81	1.97	1.87
	10	1.48	17.11	4.09	12.70
	13	1.48	8.13	3.85	14.80
	14	1.48	9.60	3.85	6.28
2-3	4	2.99	2.93	5.91	5.00
	5	3.34	3.33	4.67	7.10
	9	3.65	5.37	6.84	7.71
	10	3.66	22.75	6.23	18.55
	13	3.65	8.59	5.11	20.59

	14	3.65	10.30	6.97	7.74
5-6	4	4.48	4.47	7.76	8.41
	5	4.61	4.60	6.71	13.29
	9	4.22	4.19	6.93	6.75
	10	4.93	5.56	9.81	11.50
	13	4.94	10.37	8.28	8.78
	14	4.88	5.16	6.13	6.17

Figure 3 shows a comparison of the different nose curves of critical bus 4 under line outage 5-6 with k = 0.2, obtained by continuation power flow method using Power System Analysis Toolbox (PSAT) software and obtained by generalized curve fit method in Real Time Digital Simulation (RTDS) with five PMUs placed at buses 2, 4, 5, 6 and 9. Figure 4 shows a comparison of the different nose curves of critical bus 5 for system intact with k = 1.0, obtained by continuation power flow method using Power System Analysis Toolbox (PSAT) software and obtained by generalized curve fit method in Real Time Digital Simulation (RTDS) with five PMUs placed at buses 2, 4, 5, 6 and 9. Figure 5 shows a comparison of the different nose curves of critical bus 4 under line outage 2-3 with k = 1.0, obtained by continuation power flow method using Power System Analysis Toolbox (PSAT) software and obtained by generalized curve fit method in Real Time Digital Simulation (RTDS) with five PMUs placed at buses 2, 4, 5, 6 and 9. Figure 6 shows a comparison of the different nose curves of critical bus 9 under line outage 5-6 with k = 1.2, obtained by continuation power flow method using Power System Analysis Toolbox (PSAT) software and obtained by generalized curve fit method in Real Time Digital Simulation (RTDS) with five PMUs placed at buses 2, 4, 5, 6 and 9.

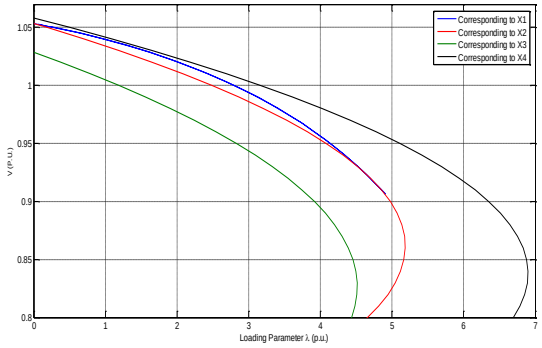

Figure 3: Nose curve of critical bus 14 for critical contingency 5-6 at k = 0.2 in IEEE 14-Bus system

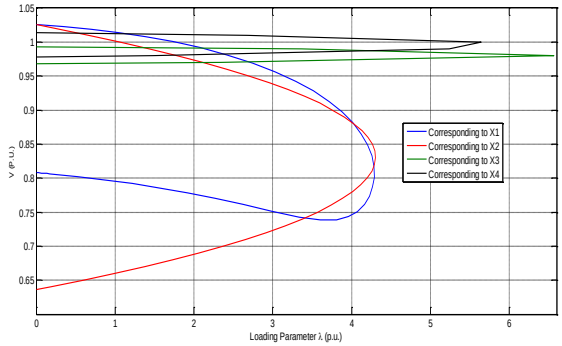

Figure 4: Nose curve of critical bus 5 for intact system at k = 1.0 in IEEE 14-Bus system

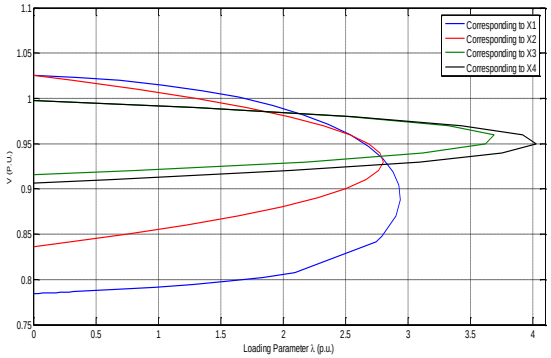

Figure 5: Nose curve of critical bus 4 for critical contingency 2-3 at *k* = 1.0 in IEEE 14-Bus system

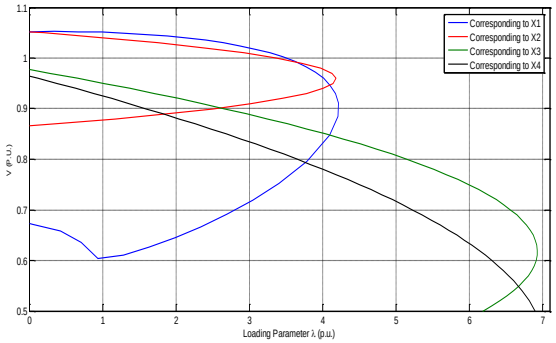

Figure 6: Nose curve of critical bus 9 for critical contingency 5-6 at *k* = 1.2 in IEEE 14-Bus system

B. NRPG 246-Bus System

In North Regional Power Grid (NRPG) of India 97 PMUs were placed to ensure complete observability by simulated consideration of all single line outages, loss of few PMUs in system and changing load patterns of the system using binary integer linear programming. Critical contingencies and critical buses for 246-Bus North Regional Power Grid (NRPG) system have also been evaluated [21]. Tables V, VI, VII and VIII show the results of voltage stability margins of different critical buses of the system in a comparative manner under different patterns of load changes (viz. *k*=0.2, 0.5, 1.0 and 1.2, respectively) obtained by continuation power flow method using Power System Analysis Toolbox (PSAT) and generalized curve fit method.

TABLE V
VOLTAGE STABILITY MARGINS COMPARISION FOR *k* =0.2 IN 246-BUS NRPG SYSTEM

Critical Contingency	Critical Bus	X_1	X_2
Intact	156	2.57	3.90
	164	2.57	3.31
	171	2.57	3.04
	173	2.57	2.81
	174	2.57	3.12
40-41	156	2.35	3.74
	164	2.35	3.14
	171	2.35	2.88
	173	2.35	2.61
	174	2.35	2.97
	156	2.60	3.91

106-123	164	2.60	3.35
	171	2.60	3.06
	173	2.60	2.84
	174	2.59	3.15
156-158	164	1.70	-
	171	1.70	2.35
	173	1.70	1.99
	174	1.70	2.45
158-160	156	2.51	3.88
	164	2.51	3.26
	171	2.51	3.01
	173	2.51	2.77
	174	2.51	3.10
160-164	156	2.52	3.86
	164	2.52	3.77
	171	2.52	3.02
	173	2.52	2.82
	174	2.52	2.98
165-171	156	2.55	3.88
	164	2.55	3.32
	171	2.55	2.85
	173	2.55	2.79
	174	2.55	3.11
168-171	156	2.56	3.89
	164	2.56	3.31
	171	1.73	1.73
	173	2.56	2.80
	174	2.56	3.14
173-174	156	2.54	3.90
	164	2.54	3.34
	171	2.54	3.05
	173	2.54	5.29
	174	1.34	1.29
181-158	156	2.26	3.77
	164	2.26	3.27
	171	2.26	2.89
	173	2.26	2.64
	174	2.26	2.98
219-77	156	2.55	3.89
	164	2.55	3.34
	171	2.55	3.02
	173	2.55	2.79
	174	2.55	3.11

TABLE VI
VOLTAGE STABILITY MARGINS COMPARISION FOR *k* =0.5 IN 246-BUS NRPG SYSTEM

Critical Contingency	Critical Bus	X_1	X_2
Intact	156	2.61	6.11
	164	2.61	3.73
	171	2.61	3.15
	173	2.61	2.93
	174	2.61	3.24
40-41	156	1.24	5.04
	164	1.24	2.70
	171	1.24	2.21
	173	1.24	1.70
	174	1.24	2.35
106-123	156	2.34	5.98
	164	2.34	3.49
	171	2.34	2.97
	173	2.34	2.69
	174	2.34	3.07
156-158	164	1.70	2.98
	171	1.70	2.53
	173	1.70	2.11
	174	1.70	2.65
158-160	156	2.60	6.09
	164	2.60	3.64
	171	2.60	3.15
	173	2.60	2.93
	174	2.60	3.24
160-164	156	2.57	6.13
	164	2.57	4.03
	171	2.58	3.15
	173	2.57	2.97
	174	2.57	3.10
165-171	156	2.60	6.10
	164	2.60	3.62
	171	2.59	2.84
	173	2.60	2.92
	174	2.59	3.22
168-171	156	2.61	6.16
	164	2.61	3.67
	171	1.59	1.59
	173	2.61	2.92
	174	2.61	3.25
173-174	156	2.58	6.15
	164	2.58	3.65
	171	2.58	3.18
	173	2.58	5.98

	174	1.21	1.21
181-158	156	2.60	6.10
	164	2.60	3.74
	171	2.60	3.15
	173	2.60	2.93
	174	2.60	3.23
219-77	156	2.27	5.96
	164	2.27	3.40
	171	2.27	2.93
	173	2.27	2.63
	174	2.27	3.03

TABLE VII
VOLTAGE STABILITY MARGINS COMPARISION FOR *k* =1.0 IN 246-BUS NRPG SYSTEM

Critical Contingency	Critical Bus	X_1	X_2
Intact	156	2.61	6.68
	164	2.61	4.19
	171	2.61	3.17
	173	2.61	3.07
	174	2.61	3.20
40-41	156	1.24	5.67
	164	1.24	2.99
	171	1.24	2.43
	173	1.24	1.91
	174	1.25	2.56
106-123	156	2.34	6.65
	164	2.34	4.03
	171	2.34	3.03
	173	2.34	2.84
	174	2.34	3.08
156-158	164	1.70	3.65
	171	1.70	2.68
	173	1.70	2.30
	174	1.70	2.78
158-160	156	2.60	6.73
	164	2.60	4.12
	171	2.60	3.17
	173	2.60	3.06
	174	2.60	3.20
160-164	156	2.57	6.73
	164	2.57	4.12
	171	2.57	3.17
	173	2.57	3.14
	174	2.56	3.08
	156	2.60	6.65
	164	2.60	4.19

165-171	171	2.59	2.67
	173	2.60	3.06
	174	2.59	3.19
168-171	156	2.60	6.64
	164	2.61	4.11
	171	1.38	1.38
	173	2.61	3.06
	174	2.60	3.21
173-174	156	2.58	6.60
	164	2.58	4.19
	171	2.58	3.19
	173	2.58	6.34
	174	1.03	1.02
181-158	156	2.60	6.71
	164	2.60	4.24
	171	2.59	3.17
	173	2.60	3.06
	174	2.59	3.19
219-77	156	2.27	6.39
	164	2.27	3.96
	171	2.27	3.00
	173	2.27	2.79
	174	2.27	3.05

TABLE VIII
VOLTAGE STABILITY MARGINS COMPARISION FOR *k* =1.2 IN 246-BUS NRPG SYSTEM

Critical Contingency	Critical Bus	X_1	X_2
Intact	156	2.58	6.68
	164	2.58	3.69
	171	2.58	3.14
	173	2.58	2.60
	174	2.17	2.17
40-41	156	2.16	6.46
	164	2.16	3.45
	171	2.16	2.95
	173	2.16	2.27
	174	2.14	2.12
106-123	156	2.55	6.72
	164	2.55	3.66
	171	2.55	3.13
	173	2.55	2.58
	174	2.17	2.17
156-158	164	2.40	3.59
	171	2.40	3.06
	173	2.40	2.46
	174	2.17	2.17

158-160	156	2.57	6.70
	164	2.57	3.64
	171	2.57	3.14
	173	2.57	2.60
	174	2.17	2.17
160-164	156	2.52	6.68
	164	2.52	4.06
	171	2.52	3.14
	173	2.52	2.56
	174	2.14	2.14
165-171	156	2.56	6.72
	164	2.56	3.66
	171	2.55	2.57
	173	2.56	2.57
	174	2.17	2.12
168-171	156	2.57	6.72
	164	2.58	3.64
	171	1.30	1.30
	173	2.57	2.60
	174	2.17	2.17
173-174	156	1.54	6.28
	164	1.54	2.94
	171	1.54	2.75
	173	1.54	5.86
181-158	156	2.56	6.68
	164	2.56	3.71
	171	2.56	3.14
	173	2.56	2.59
	174	2.17	2.17
219-77	156	2.50	6.69
	164	2.50	3.66
	171	2.50	3.11
	173	2.50	2.54
	174	2.17	2.17

In generalized curve fit method the first point corresponds to base case point (λ=0) while the other two points are found using two steps of continuation power flow method near but before critical point. These three points for use in generalized curve fit method were obtained from nose curve (V-λ curve) by utilizing data obtained from pseudo-measurements and PMUs measurements by continuation power flow method using Power System Analysis Toolbox (PSAT). As seen from Tables V, VI, VII and VIII the voltage stability margins X_1 and X_2 are different but this difference in magnitudes of X_1 and X_2 may not be considered marginal for most of the critical buses considering wide patterns of load increase (viz. k=0.2, 0.5, 1.0 and 1.2 respectively). Therefore, the performance of generalized curve fit method using PMUs in the system is fairly good compared to benchmark continuation power flow results.

Figure 7 shows a comparison of the nose curves (V-λ) corresponding to voltage stability margins X_1 and X_2 of critical bus 171 under critical contingency 40-41 for k=0.2 and Figure 8 also shows a comparison of the nose curves (V-λ) corresponding to voltage stability margins X_1 and X_2 of critical bus 173 under critical contingency 160-164 for k=0.5. Figure 9 compares the nose curves (V-λ) corresponding to voltage stability margins X_1 and X_2 of critical bus 174 under critical contingency 173-174 for k=1.0. While Figure 10 shows a comparison of the nose

curves (V-λ) corresponding to voltage stability margins X_1 and X_2 of critical bus 164 under critical contingency 168-171 for k=1.2.

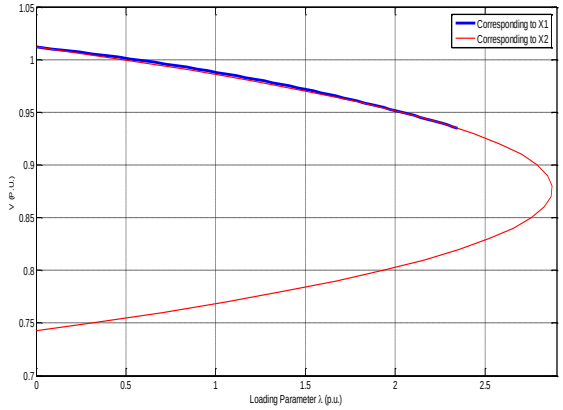

Figure 7: Nose curve of critical bus 171 under line outage 40-41 with k = 0.2 (NRPG 246-bus system)

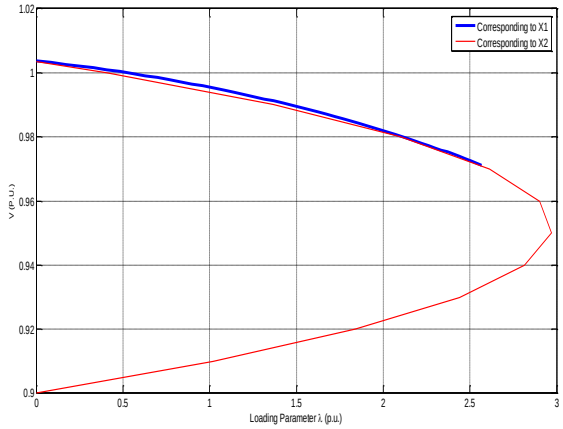

Figure 8: Nose curve of critical bus 173 under line outage 160-164 with k = 0.5 (NRPG 246-bus system)

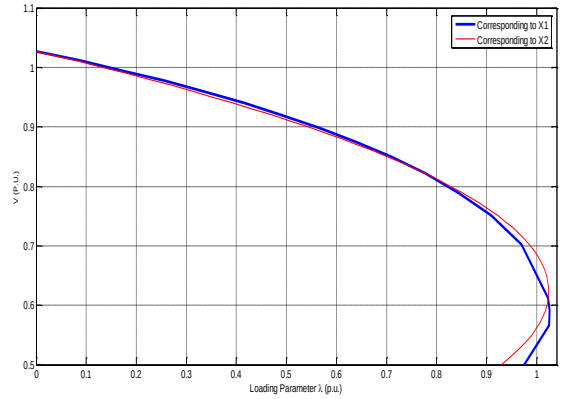

Figure 9: Nose curve of critical bus 174 under line outage 173-174 with k = 1.0 (NRPG 246-bus system)

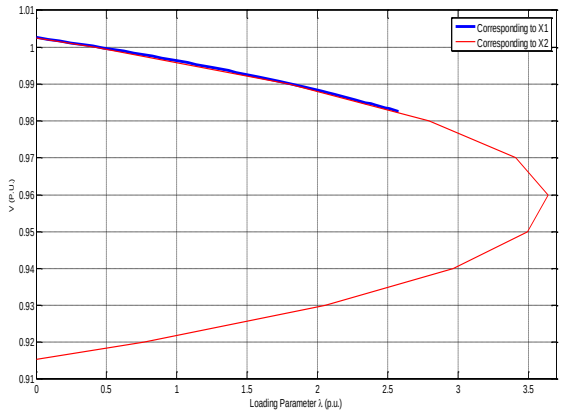

Figure 10: Nose curve of critical bus 164 under line outage 168-171 with *k* = 1.2 (NRPG 246-bus system)

Voltage stability margin X_1 gives the voltage stability information of the system using Power System Analysis Toolbox (PSAT) by continuation power flow method with 97 PMUs placed in the system. Voltage stability margin X_2 gives the voltage stability information of the system using generalized curve fit method where three points of nose curve were used to trace a second order polynomial. .

Conclusions

In this paper, the proposed generalized curve fit method using PMU measurements is used to estimate voltage stability of the system. Voltage stability margin obtained by proposed generalized curve fit method using PMU in the system under changing load patterns have been compared with the voltage stability margin obtained by continuation power flow method. Voltage stability margin obtained using generalized curve fit method and continuation power flow method match with each other. Generalized curve fit method does not require to compute and trace *V*-λ curve like continuation power flow method rather three points are used to compute a good equivalent voltage stability margin. Nose curves obtained using generalized curve fit and continuation power flow methods are also compared with each other. Results of simulations on IEEE 14-bus system and a practical 246-bus Northern Regional Power Grid (NRPG) system of India validate effectiveness of proposed generalized curve fit approach using PMU in voltage stability estimation under contingencies at different load patterns.

APPENDIX A

Critical contingencies of the system may change with the changes in operating conditions of the system. In order to consider impact of changing operating conditions in selection of critical contingencies, Voltage Stability Margin has been calculated under contingencies considering wide patterns of load increase by varying real and reactive power demands at buses as per following:

$$P_{D_i} = P_{D_{ib}}(1+\lambda) \quad (1)$$

$$Q_{D_i} = kQ_{D_{ib}}(1+\lambda) \quad (2)$$

where,

P_{D_i} = Real power demand at bus *i*

Q_{D_i} = Reactive power demand at bus *i*

$P_{D_{ib}}$ =Real power demand at bus *i* at the base case operating point

$Q_{D_{ib}}$ =Reactive power demand at bus *i* at the base case operating point

λ = System loading factor common to all the buses

k = A multiplier used to change Q_{Di}/P_{Di} ratio to consider different patterns of load increase

In order to consider wide variations in operating conditions, the multiplier *k* has been taken as 0.2, 0.5, 1.0 and 1.2, respectively.

APPENDIX B

X_1 = Voltage Stability Margin (distance between base case operating point and maximum loadability point) of the system with load variation in one critical bus only and keeping other bus voltages constants at rated values (obtained after running continuation power flow using PSAT Software using PMUs in the system)

X_2 = Voltage Stability Margin (distance between base case operating point and maximum loadability point) of the system with load variation in one critical bus only and keeping other bus voltages constants at rated values (obtained by generalized curve fit method in PSAT Software using PMUs in the system)

X_3 = Voltage Stability Margin (distance between base case operating point and maximum loadability point) of the system with load variation in one critical bus only and keeping other bus voltages constants at rated values (obtained by generalized curve fit method in RTDS using PMUs in the system)

X_4 = Voltage Stability Margin (distance between base case operating point and maximum loadability point) of the system with load variation in one critical bus only (obtained by generalized curve fit method in RTDS using PMUs in the system) [21]

References

[1] Jaime De La Ree, V. Centeno, J. S. Thorp and A. G. Phadke "Synchronized Phasor Measurement Applications in Power Systems," *IEEE Trans. on Smart Grid,* vol. 1, no. 1, pp. 20-27, April 2010.
[2] P. Kundur, *Power System Stability and Control,* New York, NY, USA: McGraw-Hill, 1994.
[3] Haoen Li, Anjan Bose and V. Venkatasubramanian, "Wide-Area Voltage Monitoring and Optimization," *IEEE Trans. on Smart Grid,* vol. 7, no. 2, pp. 785-793, March 2016.
[4] M. Parniani, J.H. Chow, L. Vanfretti, B. Bhargawa and A. Salazar, "Voltage Stability Analysis of a Multiple-Infeed Load Centre using Phase Measurement Data," *in Proceedings of Power System Conference and Exposition,* pp. 1299-1305, 29 October-1 November 2006, Atlanta, GA, USA.
[5] I. Smon, G. Verbic and F. Gubina, "Local Voltage Stability Index using Tellegen's Theorem," *IEEE Trans. on Power Systems,* vol. 21, no. 3, pp. 1267-1275, August 2006.
[6] M. Glavic and T. Van Cutsem, "Wide-Area Detection of Voltage Instability from Synchronized Phasor Measurements. Part I: Principle," *IEEE Trans. on Power Systems,* vol. 24, no. 3, pp. 1408-1416, August 2009.
[7] M. Glavic and T. Van Cutsem, "Wide-Area Detection of Voltage Instability from Synchronized Phasor Measurements. Part II: Simulation Results," *IEEE Trans. on Power Systems,* vol. 24, no. 3, pp. 1417-1425, August 2009.
[8] S. M. Abdelkader and D. J Morrow, "Online Tracking of Thevenin Equivalent Parameters using PMU Measurements," *IEEE Trans. on Power Systems,* vol. 27, no. 2, pp. 975-983, May 2012.
[9] S. Corsi and G. N. Taranto, "A Real-Time Voltage Instability Identification Algorithm Based on Local Phasor Measurements," *IEEE Trans. on Power Systems,* vol. 23, no. 3, pp. 1271-1279, August 2008.
[10] Fengkai Hu, Kai Sun, Alberto Del Rosso, Evangelos Farantatos and Navin Bhatt, "Measurement-Based Real-Time Voltage Stability Monitoring for Load Areas," *IEEE Trans. on Power Systems,* vol. 31, no. 4, pp. 2787-2798, July 2016.
[11] Xing Liu, Xun Zhang and V. Venkatasubramanian, "Distributed Voltage Security Monitoring in Large Power Systems using Synchorphasors," *IEEE Trans. on Smart Grid,* vol. 7, no. 2, March 2016.
[12] H. Khoshkhoo and S. Shahrtash, "Online Dynamic Voltage Instability Prediction Based on Decision Tree Supported by a Wide-Area Measurement System," *IET, Generation, Transmission and Distribution,* vol. 6, no. 11, pp. 1143-1152, November 2011.

[13] V. Ajjarapu, C. Christy, "The Continuation Power Flow: A Tool for Steady State Voltage Stability Analysis," *IEEE Trans. on Power Systems, vol.* 7, no. 1, pp. 416-423, February 1992.
[14] C. Canizares and F. Alvarado, "Point of Collapse and Continuation Methods for Large ac/dc Systems," *IEEE Trans. on Power Systems,* vol. 8, no. 1, pp. 1-8, February 1993.
[15] B. Milosevic and M. Begovic, "Voltage Stability Protection and Control using a Wide-Area Network of Phasor Measurements," *IEEE Trans. on Power Systems,* vol. 18, no. 1, pp. 121-127, February 2003.
[16] S. Ghiocel and J. Chow, "A Power Flow Method using a New Bus Type for Computing Steady-State Voltage Stability Margins," *IEEE Trans. on Power Systems,* vol. 29, no. 2, pp. 958-965, March 2014.
[17] Costas D. Vournas, Charalambos Lambrou and Marios Kanatas, "Application of Local Autonomous Protection Against Voltage Instability to IEEE Test Systems," *IEEE Trans. on Power Systems,* vol. 31, no. 4, July 2016.
[18] Yiwei Qiu, Hao Wu, Yongzhi Zhou and Yonghua Song, "Global Parametric Polynomial Approximation of Static Voltage Stability Region Boundaries," *IEEE Trans. on Power Systems,* vol. 32, no. 3, pp. 2362-2371, May 2017.
[19] G. C. Ejebe, G. D. Irisarri, S. Mokhtari, O. Obadina, P. Ristanovic and J. Tong, "Methods for Contingency Screening and Ranking for Voltage Stability Analysis of Power Systems," *IEEE Trans. on Power Systems,* vol. 11, no. 1, pp. 350-356, February 1996.
[20] North Region Power Grid (NRPG) 246-Bus System; 2013 [Available: http://www.iitk.ac.in/eeold/facilities/Research_labs/Power_System/NRPG-DATA.pdf].
[21] Pankaj Sahu and M. K. Verma, "Optimal Placement of PMUs in Power System Network for Voltage Stability Estimation under Contingencies," *IEEE International Conference on Computer Applications in Electrical Engineering – Recent Advances (CERA - 2017),* 5-7 October 2017.
[22] IEEE 14-Bus System; [Available: http://www.ee.washington.edu/research/pstca/pf14/pg_tca14bus.htm].
[23] Ranjana Sodhi, S. C. Srivastava and S. N. Singh, "Optimal PMU Placement to Ensure System Observability under Contingencies," *IEEE Power and Energy Society General Meeting (PES'09),* pp. 1-6, July 26-30, 2009, Calgary, Canada.